Sonochemical synthesis of cobalt aluminate nanoparticles under various preparation parameters

Weizhong Lv *, Qi Qiu, Fang Wang, Shaohui Wei, Bo Liu, Zhongkuan Luo

College of Chemistry and Chemical Engineering, Shenzhen University, Shenzhen 518060, PR China

ABSTRACT

Cobalt aluminate ($CoAl_2O_4$) nanoparticles were synthesized using a precursor method with the aid of ultrasound irradiation under various preparation parameters. The effects of the preparation parameters, such as the sonochemical reaction time and temperature, precipitation agents, calcination temperature and time on the formation of $CoAl_2O_4$ were investigated. The precursor on heating yields nanosized $CoAl_2O_4$ particles and both these nanoparticles and the precursor were characterized by means of X-ray diffraction (XRD), scanning electron microscopy (SEM), transmission electron microscopy (TEM) and atomic force microscopy (AFM). The use of ultrasound irradiation during the homogeneous precipitation of the precursor reduces the duration of the precipitation reaction. The mechanism of the formation of cobalt aluminate was investigated by means of Fourier transformation infrared spectroscopy (FT-IR) and EDX (energy dispersive X-ray). The thermal decomposition process and kinetics of the precursor of nanosized $CoAl_2O_4$ were investigated by means of differential scanning calorimetry (DSC) and thermogravimetry (TG). The apparent activation energy (E) and the pre-exponential constant (A) were 304.26 kJ/mol and $6.441 \times 10^{14} \, s^{-1}$, respectively. Specific surface area was investigated by means of Brunauer Emmett Teller (BET) surface area measurements.

© 2010 Elsevier B.V. All rights reserved.

1. Introduction

Sonochemistry is the research area in which molecules undergo a chemical reaction due to the application of powerful ultrasound radiation (20 kHz to 10 MHz) [1–3]. The physical phenomenon responsible for the sonochemical process is acoustic cavitation. Recently, the sonochemical methods, i.e. chemical reaction of the starting materials in the presence of an applied high frequency ultrasonic waves, has been employed for several purposes, in various organic and inorganic reactions and also fabrication of nanostructured materials, including the synthesis of ferrite and aluminate nanostructured materials [4–6]. The effect of ultrasound in chemical reactions is not well understood. However, it is mostly believed that during sonication, the acoustic cavitation phenomenon generates in the liquid solution of the reactants. The cavitation processes consist of the creation, growth and implosive collapse of gas vacuoles in the solution. According to the "hot-spot" theory, extreme temperatures (>5000 K) and high pressures (>20 Mpa) and cooling rates (>$10^{10} \, K \, s^{-1}$) occur within the bubbles during cavitational collapse [7]. Under such extreme conditions the solvent molecules undergo hemolytic bond cleavage to generate radicals, for example, H· and OH· when H_2O is sonicated [8,9]. These

conditions have been effectively used to prepare nanoscale metals, metal oxides and nanocomposites [10–13]. The sonochemical method has some advantages, including uniformity of mixing, reduction of crystal growth and morphological control. Ultrasound can also fracture agglomerates to produce a uniform composition of products [14]. The use of ultrasound radiation, during the homogeneous precipitation of the precursor, is expected to reduce the duration of the precipitation reaction of the precursor and to ensure homogeneity of the cations in the precursor [15]. The librated radicals, therefore, may lead to various chemical and physical effects in reaction pathways and mechanisms. Moreover, the other benefit in using ultrasonic waves in reactions is believed to be the provision of high-intensive mixing especially in viscous medias [16]. This would lead to an acceleration effect in chemical dynamics and rates of the reactions. Therefore, by this circumstance, different properties of the final product, namely, particle size, shape and its purity would be under the control of a series of factors such as sonication output power, temperature, time, solvent, chemical species and their concentrations in the reaction mixture.

Cobalt aluminate ($CoAl_2O_4$) is a thermally and chemically stable pigment of intense blue color (Thenard's blue), which has been widely used for the coloration of plastics, paint, fibers, paper, rubber, phosphor, glass, cement, glazes, ceramic bodies and porcelain enamels. It exhibits the normal spinel structure and is used for color TV tubes as contrast-enhancing luminescent pigments [17–19].

---

* Corresponding author. Tel.: +86 755 26557249; fax: +86 755 26536141.
E-mail address: weizhonglv@163.com (W. Lv).

Cobalt aluminate has been paid attention to as an advanced pigment because of its technological significance [20]. The pigment material with fine particle size, nonaggregation, and a narrow size distribution is known to have good reflective characteristics in terms of its contrast-enhancing luminescence. Particularly, the particle morphology can influence the optical property of the pigment. The spherical morphology of pigments is required for high-reflectivity, because pigment particles with spherical morphology decrease the scattering of the light from pigment surfaces [21–23]. Recently, $CoAl_2O_4$ has been prepared with a number of methods, such as co-precipitation [24,25], sol–gel [26–31], hydrothermal synthesis [32,33] and low temperature combustion [34]. However, the co-precipitation method requires enormous effort to ensure a homogeneous material with uniform particle size and composition. Also, by using this method, aluminium oxide often crystallizes as a by-product. Using the sol–gel method, the elements become uniformly distributed during the gel formation step. However, the disadvantages of the sol–gel process are the relative high cost of the metal alkoxides and the release of large amounts of alcohol during the calcination step which requires safety considerations. The sonochemical method is superior to all of the other techniques mentioned above. However, no literature precedence, to our knowledge, is available on the synthesis of $CoAl_2O_4$ by the sonochemical method. Hence, studying with the sonochemical method, the synthesis of nanosized cobalt aluminate particles will be worthwhile.

Previous authors [35–41] have synthesized a series of aluminates or ferrites using the sonochemical method. In the present work, $CoAl_2O_4$ nanoparticles were synthesized by the sonochemical method with the starting materials $Co(NO_3)_2 \cdot 6H_2O$ as the source of Co and $Al(NO_3)_3 \cdot 9H_2O$ as the source of Co and Al, respectively. During the synthesis, the effect of preparation parameters, such as the sonochemical reaction time and temperature, precipitation agents, calcination temperature and time was studied on the purity, particle size and morphology of the final product using X-ray diffraction (XRD), scanning electron microscopy (SEM), transmission electron microscopy (TEM) and atomic force microscopy (AFM). The mechanism of the formation of cobalt aluminate was investigated by means of Fourier transformation infrared spectroscopy (FT-IR) and EDX (energy dispersive X-ray). The thermal decomposition process and kinetics of the precursor of nanosized $CoAl_2O_4$ were investigated using differential scanning calorimetry (DSC) and thermogravimetry (TG) and the mechanism of the formation of cobalt aluminate was obtained. Specific surface area was investigated by means of Brunauer Emmett Teller (BET) surface area measurements.

2. Experimental

2.1. Sonochemical synthesis

Sonication was performed using a SC-4 high-intensity ultrasonic reactor (Chengdu Jiuzhou Ultrasound Factory, China; 0.6 cm tip diameter, with a titanium horn operating at 20.81 kHz at a power of 100 W cm^{-2}) at room temperature. All the reagents were of reagent grade purchased from Guangzhou Chemical Reagents Factory (Guangzhou, China), and were used without further purification. The synthesis of the precursor to nanosized $CoAl_2O_4$ was carried out with the aid of ultrasound radiation. First, the precipitation agents, $Co(NO_3)_2 \cdot 6H_2O$ and $Al(NO_3)_3 \cdot 9H_2O$ in stoichiometry were added in a sonication flask, and formed a solution. Secondly, the solution was purged with argon for 15 min and irradiated with high-intensity ultrasound radiation under argon at a pre-determined temperature for a pre-determined time by employing a direct immersion horn. The pH of the solution changed from 6.1,

prior to the sonication, to 7.0 at the end of the precipitation. After the precipitation reaction was complete, the precipitate was separated from the solution by centrifugation, washed repeatedly with distilled water and ethanol, and was finally dried in a vacuum for 10 h at 110 °C. The dried product was then used as a precursor for $CoAl_2O_4$. The dried precursor was calcined at a pre-determined temperature for a pre-determined time to become nanosized $CoAl_2O_4$ particles.

2.2. Characterization

The powder X-ray diffraction patterns were recorded on a Bruker X-ray diffractometer (Model D/max-3A, CuKα, λ = 1.5418 Å, German). The morphologies of the products were examined by scanning electron microscopy (SEM, JSM-5910, Japan), transmission electron microscopy (TEM, JEM-100 CXII, Japan) and atomic force microscopy (AFM, CSPM5000, Being Nano-Instruments, China). The Cu/Al atomic ratios of the products were examined using an SEM with electron dispersive X-ray (EDX) analysis. A carbon layer was vacuum–vapor-deposited onto the samples to provide a conducting surface. FT-IR spectra were recorded on a Perkin–Elmer 1730 (American) infrared spectrophotometer with KBr pellets in the range of 400–4000 cm^{-1}. The thermogravimetric analysis was performed with a thermal analyzer (NETZSCH STA 409 PC/PG). Typically, about 25–35 mg sample was programmable-heated from room temperature to 800 °C in a N_2 atmosphere with a heating rate of 3, 5, 10, 15 and 20 °C min^{-1}, respectively. The DSC pattern was measured in the range of 30–800 °C using a Mettler Toledo (DSC-60, Japan) instrument under the nitrogen atmosphere at a heating rate of 3, 5, 10, 15 and 20 °C min^{-1}, respectively. The surface areas of the nanoparticles were measured by the BET nitrogen gas adsorption method using a Micromeritics Gemini instrument (NOVA1200e, American) with a value of 0.164 nm^2 for the cross-section of the nitrogen molecule.

3. Results and discussion

3.1. Sonochemical reaction time

The outcome of the sonochemical method is similar to that which would be achieved by chemical co-precipitation but it has some advantages, namely, uniformity of mixing, reduction in crystal growth, morphological control, reduction in agglomeration, etc. The objective of the present work is to utilize ultrasound radiation in the process of homogeneous precipitation for the synthesis of a precursor of nanosized $CoAl_2O_4$. The use of ultrasound radiation during the homogeneous precipitation of the precursor is expected to reduce the duration of the precipitation reaction of the precursor and to ensure the homogeneity of the cations in the precursor.

Fig. 1 shows the characteristic XRD pattern of $CoAl_2O_4$ which was synthesized using $Co(NO_3)_2 \cdot 6H_2O$ and $Al(NO_3)_3 \cdot 9H_2O$ as starting materials, with urea as a precipitation agent at a concentration of 9 M, ultrasound irradiation at 70 °C for 4 h and calcined at a temperature of 1000 °C for 6 h. The principal d values taken from the JCPDS 44-0160 $CoAl_2O_4$ are 2.8650 ($2\theta = 31.193°$, lattice plane of {2 2 0}), 2.4440 ($2\theta = 36.742°$, lattice plane of {3 1 1}), 2.0260 ($2\theta = 44.692°$, lattice plane of {4 0 0}), 1.8596 ($2\theta = 48.940°$, lattice plane of {3 3 1}), 1.6544 ($2\theta = 55.497°$, lattice plane of {4 2 2}), 1.5597 ($2\theta = 55.190°$, lattice plane of {5 1 1}), 1.4328 ($2\theta = 65.041°$, lattice plane of {4 4 0}), 1.2815 ($2\theta = 73.894°$, lattice plane of {6 2 0}) and 1.2359 ($2\theta = 77.108°$, lattice plane of {5 3 3}) Å. In this study, XRD peaks for the $CoAl_2O_4$ nanoparticles have been observed at d = 2.8599 ($2\theta = 31.200°$), 2.4414 ($2\theta = 36.760°$), 2.0244 ($2\theta = 44.700°$), 1.8596 ($2\theta = 48.940°$), 1.6517 ($2\theta = 55.500°$), 1.5589 ($2\theta = 59.200°$), 1.4312 ($2\theta = 65.060°$),
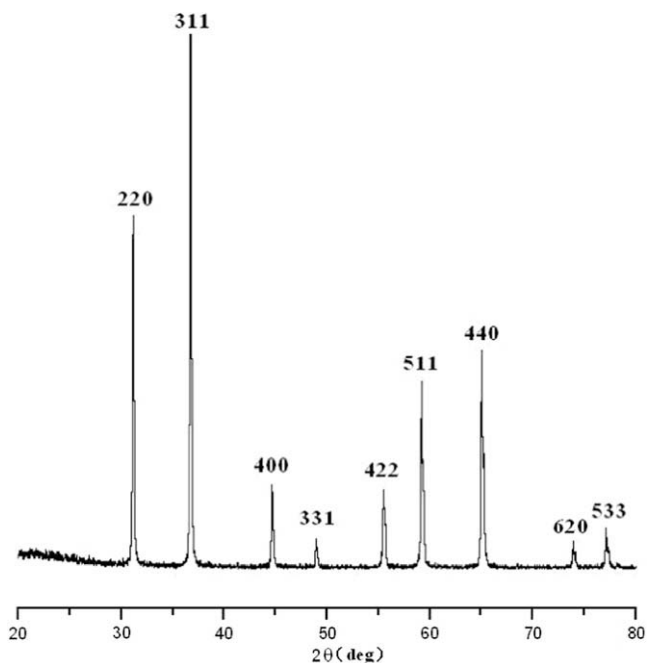
Fig. 1. XRD patterns of CoAl$_2$O$_4$ nanosized powders synthesized using Co(NO$_3$)$_2$·6H$_2$O and Al(NO$_3$)$_3$·9H$_2$O as starting materials, with urea as a precipitation agent at a concentration of 9 M, ultrasound irradiation at 70 °C for 4 h and calcination temperature 1000 °C for 6 h.

1.2823 ($2\theta = 73.920°$) and 1.2362 ($2\theta = 77.140°$) Å, which are in agreement with the JCPDS 44-0160 standard values. On the basis of the Debeye–Scherrer equation, the crystallite size was calculated to be ca. 20 nm using the (3 1 1) reflection at $d = 2.4414$ Å.

The sonochemical reaction times are the key factors in controlling the aggregation and uniformity of the product particle size. The present work studies the effect of the sonochemical reaction times on the product particle size and composition. We chose sonochemical reaction times of 0, 2 or 4 h, respectively, without changing any other parameters. The XRD patterns of cobalt aluminate powders are shown in Fig. 2 and it can be observed that as the sonochemical reaction times were increased from 0 to 4 h, crystallinity increased accordingly. However, the new peak line at $d = 1.8596$ Å (lattice plane of {3 3 1}) is clearly observed in the
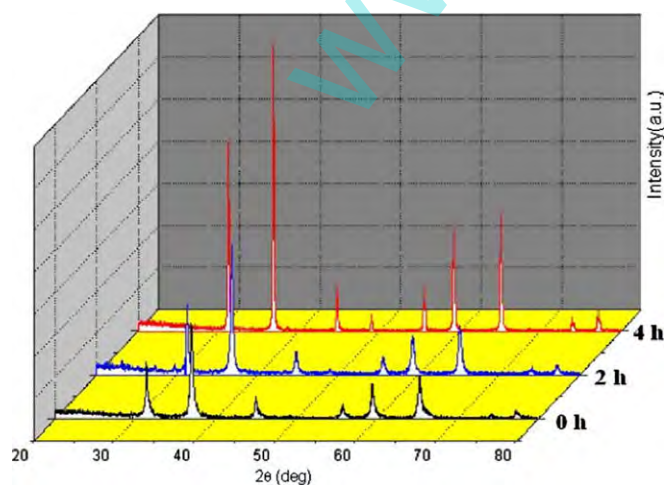
XRD patterns when the sonochemical reaction time is 4 h. Fig. 2 also showed that all the peaks are much sharper at longer sonochemical reaction time.

The TEM micrographs of the CoAl$_2$O$_4$ powders prepared at different sonochemical reaction time of 0 and 4 h are shown in Fig. 3. Fig. 3a shows that the powder prepared for 4 h consists of ultrafine, well dispersed particles with uniform particle size of 9–38 nm, and the result was in agreement with the XRD characterized result. Transmission electron micrograph of the powders indicated nonaggregated particles. Particle size distribution in TEM micrograph was fairly small. Whereas for the powders synthesized at a sonochemical reaction time of 0 h without sonication (Fig. 3b) shows that the powder consists of not well dispersed particles with particle size of 16–201 nm, and transmission electron micrograph of the powders indicated aggregated particles. The shape of the
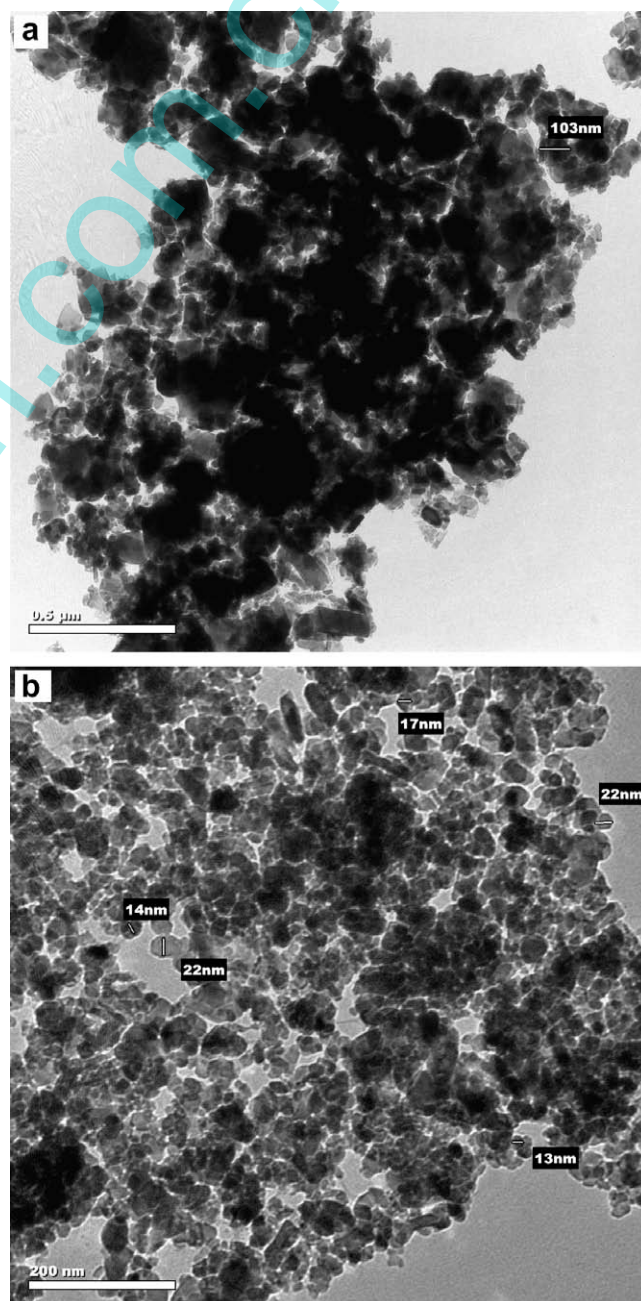

Fig. 3. TEM image of CoAl$_2$O$_4$ nanosized powders obtained at sonochemical reaction time of: (a) 0 h and (b) 4 h.

Fig. 2. XRD patterns of CoAl$_2$O$_4$ nanosized powders obtained at different sonochemical reaction time.

$CoAl_2O_4$ particles also varies with reaction time, from regularly cubical shape (Fig. 3b) to a less regular shape (Fig. 3a).

The nanosized $CoAl_2O_4$ powders were characterized by atomic force microscopy in tapping mode. The scanning area of the sample was 2×2 μm. The sample was prepared by diffusion in 95% ethanol for 15 min under ultrasonic radiation and then coating it on a muscovite substrate and dried for 30 min under atmosphere. Fig. 4 shows the AFM results of nanosized $CoAl_2O_4$ and a clear topographic image of the nanosized $CoAl_2O_4$ powders is depicted. It is seen that a clear topographic image was obtained, and that the $CoAl_2O_4$ products are nanosized powders and the particles size is uniform at about 20 nm. The three-dimensional view of the same sample (Fig. 4b) illustrates that the particle size of the $CoAl_2O_4$ powders were in the range of 8.40–21.22 nm with a small size distribution. The morphological characteristics of $CoAl_2O_4$ powders observed from the AFM images were consistent with their TEM images.

3.2. Sonochemical reaction temperature

The effect of sonochemical reaction temperature was studied on the purity and morphology of the particles. Fig. 5 shows the XRD patterns of samples synthesized at 30, 50 or 70 °C, respectively, without changing any other parameters as in Section 3.1. The re-
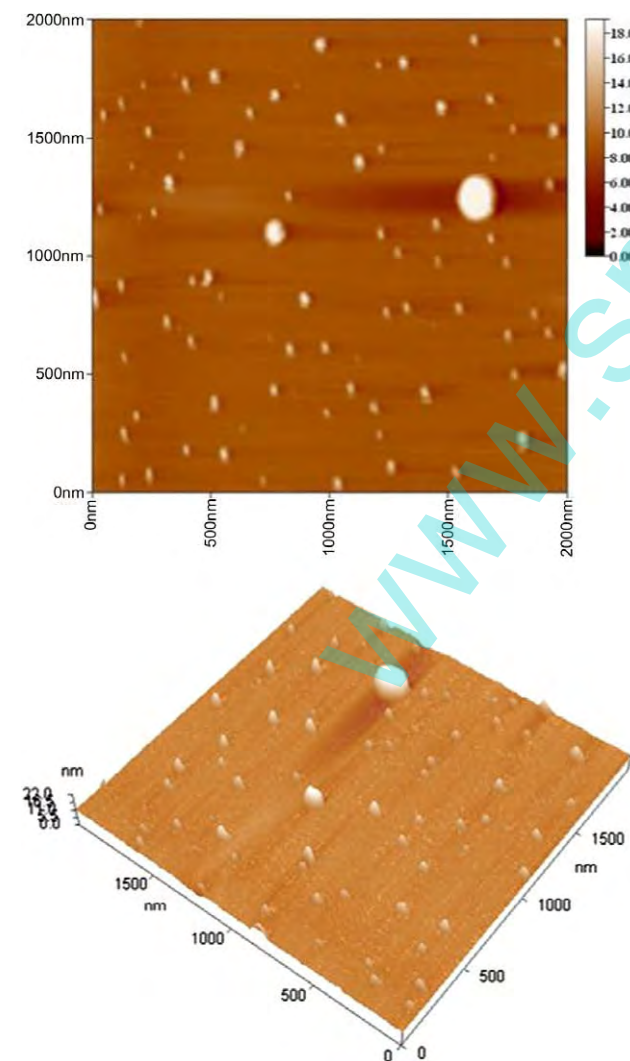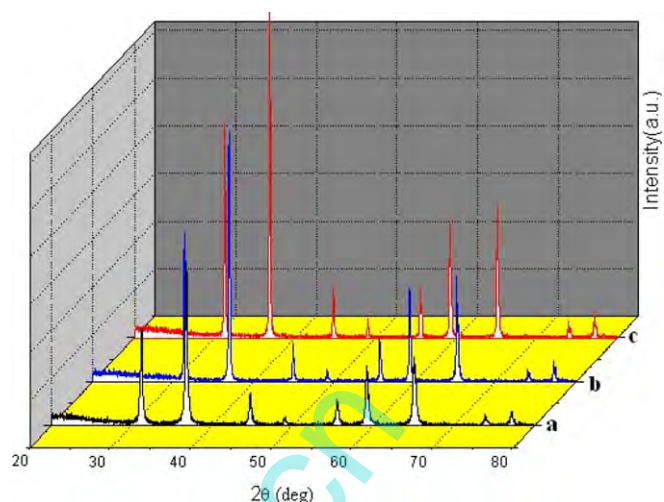

Fig. 5. XRD patterns of $CoAl_2O_4$ nanosized powders synthesized at sonochemical reaction temperature of (a) 30 °C, (b) 50 °C and (c) 70 °C.

sult shows that the three XRD patterns are characteristic of cubic structured cobalt aluminate. From Fig. 5, XRD peaks for the $CoAl_2O_4$ nanoparticles have been observed at $2\theta = 31.200°$, $36.760°$, $44.700°$, $48.940°$, $55.500°$, $59.200°$, $65.060°$, $73.920°$ and $77.140°$, which are in agreement with the JCPDS 44-0160 values. With the increase of the sonochemical reaction temperature, the peak line at $d = 1.8596$ Å (lattice plane of {3 3 1}) is more and more clearly observed in the XRD patterns. The full width at half maximum (FWHM) of the 2 2 0, 3 1 1, and 4 0 0 reflection peaks decreased with the increase in the sonochemical reaction temperature. With the increase of the sonochemical reaction temperature, crystallinity increased and particle size increased accordingly. The sonochemical method has some advantages, including uniformity of mixing, reduction of crystal growth, and morphological control. Ultrasound can also fracture agglomerates to produce a uniform composition of products. The use of ultrasound radiation during the homogeneous precipitation of the precursor is expected to reduce the precipitation time of the precursor and to ensure homogeneity of the cations in the precursor. The librated radicals therefore, may lead to various chemical and physical effects in reaction pathways and mechanisms. Moreover, the other benefit in using ultrasonic waves in reactions is believed to be providing high-intensive mixing especially in viscous sonochemical reaction temperature. This would lead to an acceleration effect in chemical dynamics and rates of the reactions.

3.3. Precipitation agents

The precipitation agents are used in all preparations of aluminates by the chemical precipitation method. To compare the composition of cobalt aluminate using the different precipitation agents, we chose NaOH, $NH_3·H_2O$ and urea as the precipitation agents, respectively, without changing any other parameters (as in Section 3.1). Fig. 6 shows the XRD patterns of cobalt aluminate prepared by using the different precipitation agents. Fig. 6c shows that the XRD pattern of cobalt aluminate prepared by using aqueous urea solution as a precipitation agent agrees well with the JCPDS 44-0160 standard data. Fig. 6b shows that the XRD pattern of cobalt aluminate prepared by using a precipitation agent, $NH_3·H_2O$, agrees with the standard data. However, the peak line at $d = 1.8596$ Å (lattice plane of {3 3 1}) is not clearly observed in the XRD patterns, and all the peaks observed are sharper for the sample synthesized by using aqueous urea solution as a precipitation agent. Fig. 6a, however, shows that the XRD pattern of cobalt
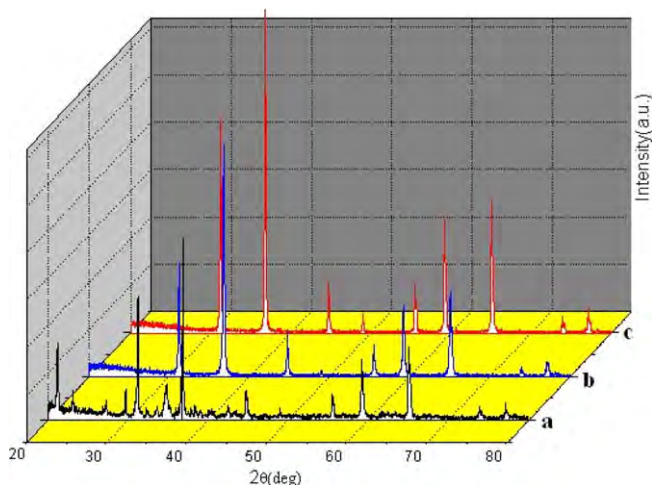

Fig. 4. AFM images of nanosize $CoAl_2O_4$ obtained at sonochemical reaction time of 4 h: (a) topographic view and (b) three-dimensional view.

Fig. 6. XRD patterns of CoAl$_2$O$_4$ nanosized powders synthesized by using (a) NaOH, (b) NH$_3$·H$_2$O and (c) urea as the precipitation agents.

Fig. 7. XRD patterns of CoAl$_2$O$_4$ nanosized powders obtained at different calcination temperature: (a) 400 °C, (b) 700 °C and (c) 1000 °C.

aluminate prepared using aqueous NaOH solution as a precipitation agent did not match well with the standard pattern. There are many peaks of impurities observed in the XRD patterns of the product prepared using aqueous NaOH solution as a precipitation agent. Urea is a very weak Bronsted base, highly soluble in water and its hydrolysis rate may be easily controlled by controlling the temperature of the reaction. Therefore using aqueous urea solution in place of NaOH can be advantageous because (a) urea does not have a tendency to get incorporated into the oxide matrix and (b) any residual urea entrained in cobalt aluminate powder can be easily removed while drying the powder at 110 °C. The role of urea in the homogeneous precipitation of the precursor is that urea decomposes by hydrolysis upon heating producing CO$_2$ gas, OH$^-$ and NH^{4+} ions in the solution. This increases the pH of the medium in a controlled manner depending on the temperature. A pH measurement revealed that the pH of the solution increased from 6.1 to 7 before and after the sonication experiment. This increase of pH is suitable for the formation of the LDH precursor. The utilization of ultrasound radiation during this homogeneous precipitation process can accelerate the process and also can be beneficial for controlling particle size in the nanoscale range. Based on the results of this research, the cobalt aluminate was synthesized successfully using aqueous urea solution as a precipitation agent.

3.4. Calcination temperature

Calcination is a necessary step in the preparation of aluminate by chemical co-precipitation. The calcination temperature plays a key role in the crystalline type and particle size of the cobalt aluminate. The cobalt aluminates were synthesized at calcination temperatures of 400, 700 or 1000 °C, respectively. All other parameters were kept the same as previously described. Fig. 7 shows different XRD patterns for the precursor calcined at different temperatures. The result shows that the three XRD patterns are characteristic of cubic structured cobalt aluminate. Cubic CoAl$_2$O$_4$ was the only phase observed in all the experiments. When the sample was calcined at a temperature higher than 700 °C, the color of the powder changed from black to bright blue. When the sample was calcined at a temperature of 1000 °C, the peak line at d = 1.8596 Å (lattice plane of {3 3 1}) is clearly observed in the XRD patterns. The XRD pattern of the sample obtained at calcinations temperature of 1000 °C showed much sharper peaks due to coarsening of the particles at higher temperature. With the increase in the calcination temperature, crystallinity increased and
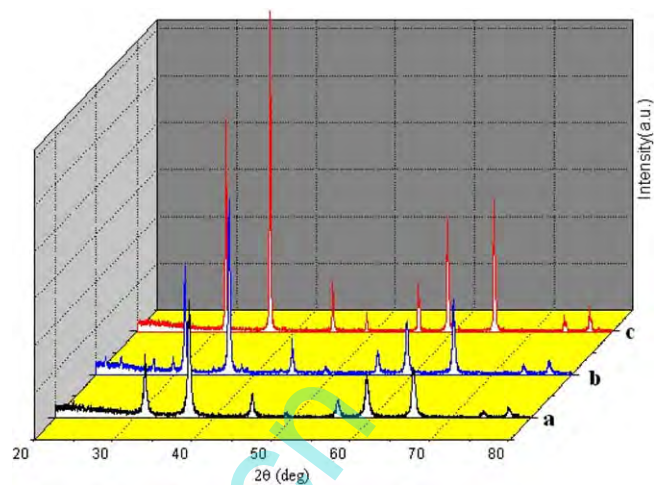
the particle sizes also increased correspondingly. There were no typical peaks when the calcination temperature was below 400 °C. According to the standard data of cobalt aluminate, the precursor calcined at 700 °C already showed a cobalt aluminate phase. The FWHM sharply decreased to 700 °C and then gradually changed. This means that the crystallinity of CoAl$_2$O$_4$ was improved with increasing treatment temperature in the temperature range studied. The powders calcined at 1000 °C showed the pure cobalt aluminate phase.

3.5. Calcination time

Calcination time has an obvious effect on the product of composition and particle size. Fig. 8 shows different XRD patterns for the powders calcined at 1000 °C for 2, 4 or 6 h, respectively, without changing any other parameters. The result shows that the three XRD patterns are characteristic of cobalt aluminate. From Fig. 10, XRD peaks for the CoAl$_2$O$_4$ nanoparticles have been observed at d = 2.8599, 2.4414, 2.0244, 1.8596, 1.6517, 1.5589, 1.4312, 1.2823 and 1.2362 Å, which are in agreement with the JCPDS 44-0160 standard values. With the increase of the calcination times, crystallinity increased and particle size increased accordingly. With the increase of the calcinations times, the peak line at d = 1.8596 Å
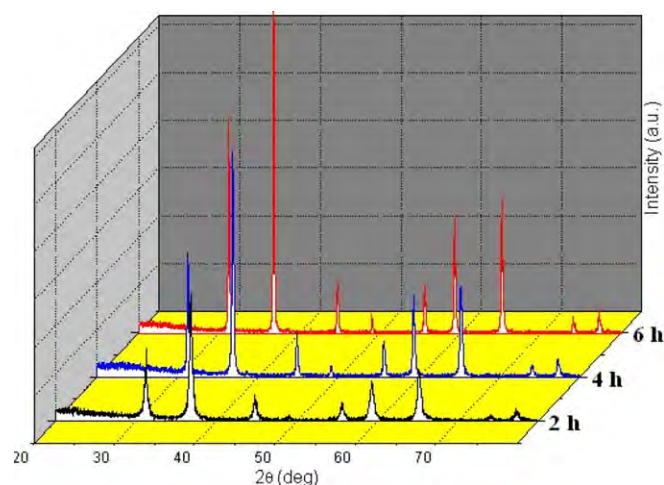

Fig. 8. XRD patterns of CoAl$_2$O$_4$ nanosized powders obtained at different calcination times.

(lattice plane of {3 3 1}) is more and more clearly observed in the XRD patterns. The FWHM of the 2 2 0, 3 1 1, and 4 0 0 reflection peaks decreased with the increase in calcination times. Therefore, the optimized cobalt aluminate formation occurs at a calcination time of 6 h.

Fig. 9a shows the results of scanning electron microscopy of $CoAl_2O_4$ before calcination. From Fig. 9a, the product exhibit a lot of aggregates, and the mean pore size is above 3 μm. Fig. 9b illustrates the results of scanning electron microscopic observation of the nanosized $CoAl_2O_4$ at a calcinations time of 6 h. The SEM micrographs show that the particle size is ca. 20 nm with little aggregation. This value is in accordance with that obtained from XRD and TEM measurements.

3.6. The mechanism of the formation of cobalt aluminate

Fig. 10 shows the IR spectra of the precursor as well as the $CoAl_2O_4$ nanoparticles. The products were synthesized using $Co(NO_3)_2·6H_2O$ and $Al(NO_3)_3·9H_2O$ as starting materials, with urea as a precipitation agent at a concentration of 9 M. The reaction was carried out at 70 °C for 4 h under ultrasound irradiation and a calcination temperature of 1000 °C for 6 h. The as-formed precursor shows the spectral features (Fig. 10a) typical of LDH, which are described in detail elsewhere [42]. The band at 3432.71 cm^{-1}, which was a strong absorption band, is attributed to the OH stretching mode, [δ(OH)]. The band at ca. 1631 cm^{-1} is assigned to the bend-ing vibrational mode of the interlayer water molecules. The weak absorption band at ca. 2190 cm^{-1} has been attributed to the existence of intercalated NH_3 species as reported in the literature [43]. The IR spectrum provides the evidence for the presence of intercalated carbonate ions. The strong absorption band at 1384.39 cm^{-1} originates from the v_3 mode of CO_3^{2-} ion. The IR bands observed below 1000 cm^{-1} can be attributed to the v_2 mode of carbonate and the M–OH modes (M = Co and Al). The precursor after heating at 1000 °C shows IR peaks at 3430.29, 667.43 and 561.90 cm^{-1}. The bands of 561.90 and 667.43 cm^{-1} arose from the CoO_4 and AlO_6 vibrations (Fig. 10b) [32].

Fig. 11 shows the results of the EDX (energy dispersive X-ray). From the elemental analysis in combination with the results obtained from EDX, the stoichiometry of the precursor heated at 1000 °C for 6 h was found to be 30.02% (weight percent) of Co, 31.00% of Al and 38.98% of O. This result theoretically agreed with the weight percent (Co 33.32%, Al 30.51% and O 36.18%). From the elemental analysis in combination with the results obtained from EDX measurements, the stoichiometry of the precursor was found to be $[Co_{0.48}Al_{0.52}(OH)_2](CO_3)_{0.26}(NH_3)_{0.13}(H_2O)_{1.2}$. The carbonate content was calculated from the Co/Al ratio, assuming carbonate is the only interlayer anion balancing the positive charge in the layers because of the presence of aluminium. The presence of interlayer CO_3^{2-}, NH_3 and H_2O, is supported by IR measurements as discussed above, and further supported by TG/DSC measurements as discussed below. According to these results, the mechanism of the formation of cobalt aluminate is obtained. The process includes four steps. First, urea was hydrolyzed and ammonia was obtained. Secondly, OH^- was formed from the ammonia. Then CO_3^{2-} and $[Co_{0.48}Al_{0.52}(OH)_2](CO_3)_{0.26}(NH_3)_{0.13}(H_2O)_{1.2}$ were yielded in turn. Finally, nanosized $CoAl_2O_4$ was synthesized after the calcination of $[Co_{0.48}Al_{0.52}(OH)_2](CO_3)_{0.26}(NH_3)_{0.13}(H_2O)_{1.2}$.

3.7. The thermal decomposition process and kinetics of the precursor of nanosized $CoAl_2O_4$

The TG pattern (heating rate of 10 °C min^{-1}) of the as-formed precursors when the sample obtained with urea as a precipitation agent (Fig. 12a) reveals weight loss steps at 89, 232 and 268 °C with an overall weight loss of 22.9%. The first two weight loss steps were attributed to the loss of physisorbed and interlayer water, respectively, and the third weight loss was ascribed to the loss of structural water, CO_2, and NH_3 from the interlayer because of the destruction of layered structure (i.e. decarbonation and dehydroxylation). The TG pattern also reveals weight loss steps at ca. 700 °C with an overall weight loss of 34.6%. At this step, pure nanosized $CoAl_2O_4$ was obtained. The DSC pattern (heating rate of 10 °C min^{-1}) of the precursor (Fig. 12b) shows irreversible endothermic peaks at 76, 238 and 261 °C. The positions of these peaks coincide well with that of the decomposition steps observed in the TG pattern. The DSC patterns (heating rate of 3, 5, 15 and 20 °C min^{-1}, respectively) of the precursor can also be obtained.

There are at least 21 different methods based on the differential equation to calculate the thermal decomposition kinetics of solid. We chose the Kissinger–Akahira–Sunose (KAS) method to solve the differential equation. The Kissinger equation is listed as Eq. (1).

$$\ln\left(\frac{\beta_i}{T_{pi}^2}\right) = \ln\frac{AR}{E} - \frac{E}{RT_{pi}}, \quad i = 1, 2, 3, 4, \ldots \tag{1}$$

where β_i is the heating rate, T_p is the peak temperature, A is the preexponential constant, E is the apparent activation energy, and $R = 8.314$ J mol/K. According to the DSC pattern recorded under different heating rates, T_p can be obtained (Table 1). A graph can be made from $\ln\left(\frac{\beta_i}{T_{pi}^2}\right) - \frac{1}{T_{pi}}$ and the line can be obtained by the method
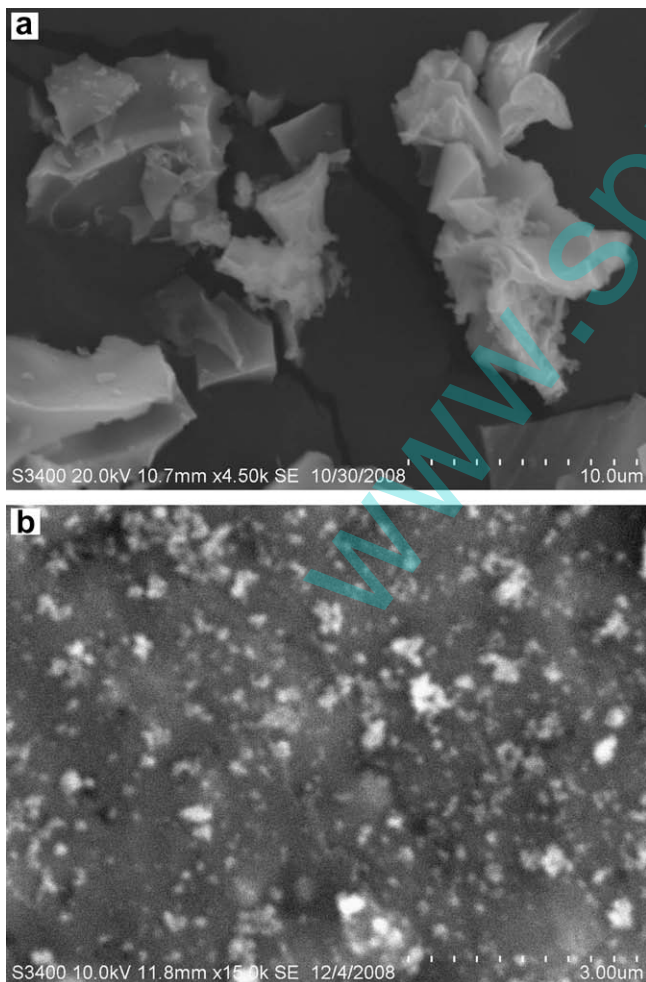
Fig. 9. SEM image of the $CoAl_2O_4$ samples obtained (a) before and (b) after calcination times of 6 h.
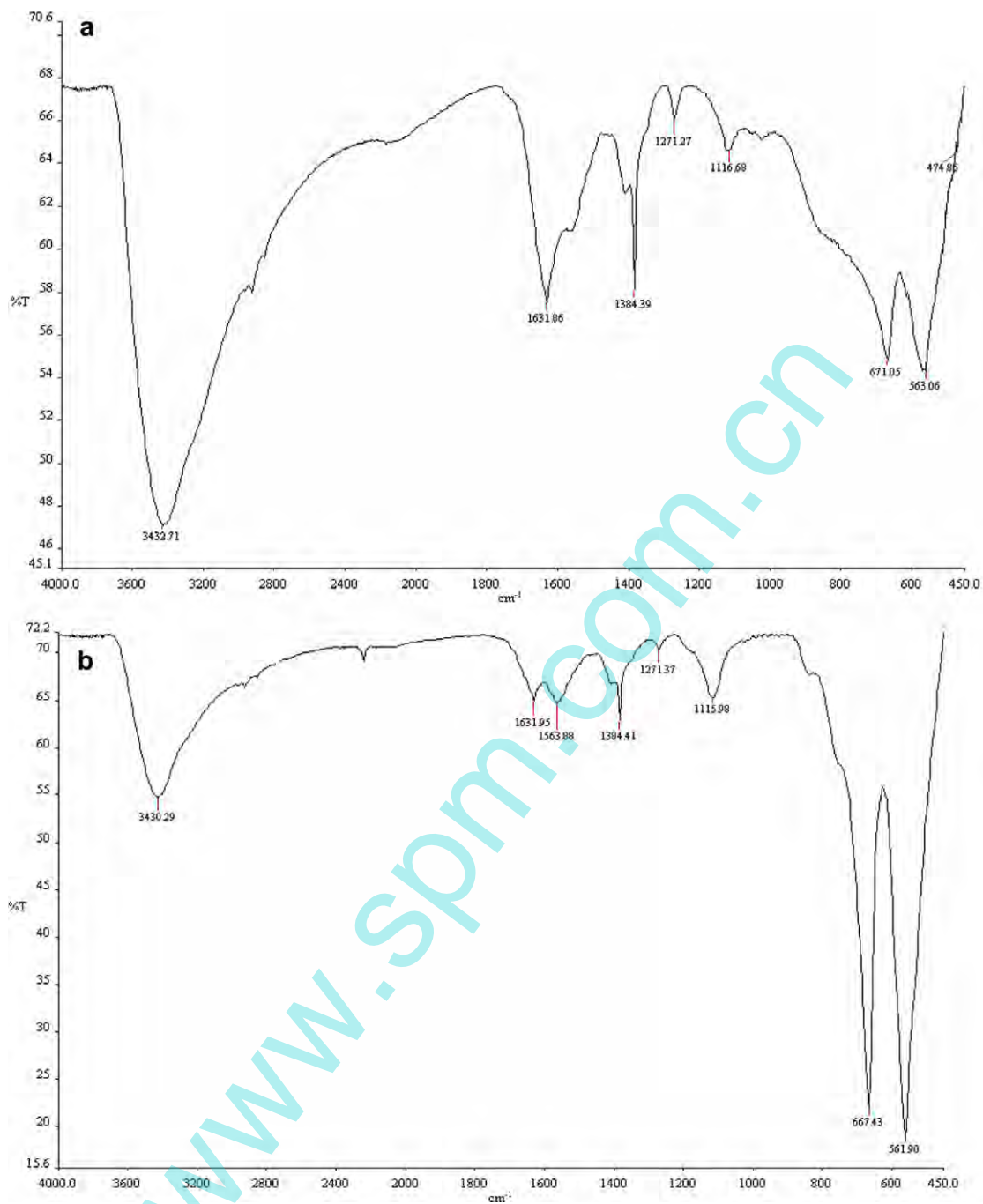
Fig. 10. IR spectrum of: (a) as-formed precursor and (b) CoAl$_2$O$_4$ nanosized powders obtained by heating the precursor at 1000 °C.
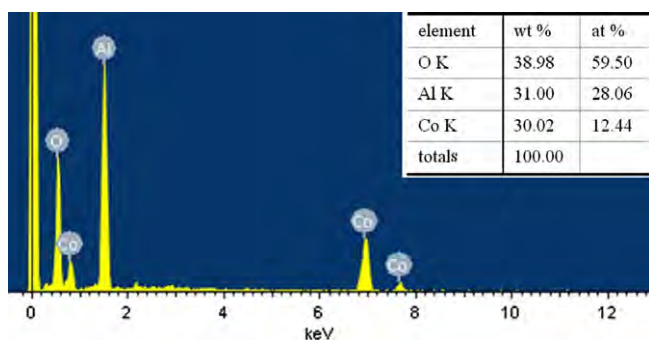

element	wt %	at %
O K	38.98	59.50
Al K	31.00	28.06
Co K	30.02	12.44
totals	100.00	

Fig. 11. EDX of CoAl$_2$O$_4$ nanosized powders.

of linear curve fit (Fig. 13). E_k is calculated from the slope of the line and A_k is calculated from the intercept of the line. As a result, the apparent activation energy (E) is 304.26 kJ/mol and the pre-exponential constant (A) is $6.441 \times 10^{14}\,\text{s}^{-1}$. The R of the fit line is 0.9962.

3.8. Specific surface area measurements

Specific surface area was measured by nitrogen adsorption–desorption BET. Table 2 reports the specific surface area values. It can be observed that specific surface area decreases with increasing calcination temperature.
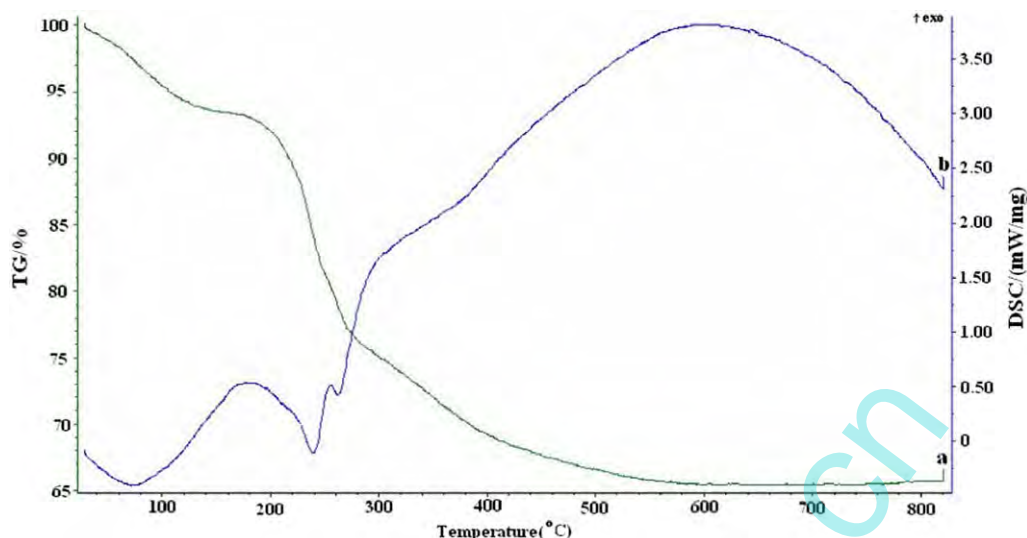
Fig. 12. (a) TG pattern of the as-formed precursor and (b) DSC pattern of the precursor obtained by using urea as a precipitation agent.

Table 1
Peak temperature at DSC curves of the precursor at different raising temperature rates.

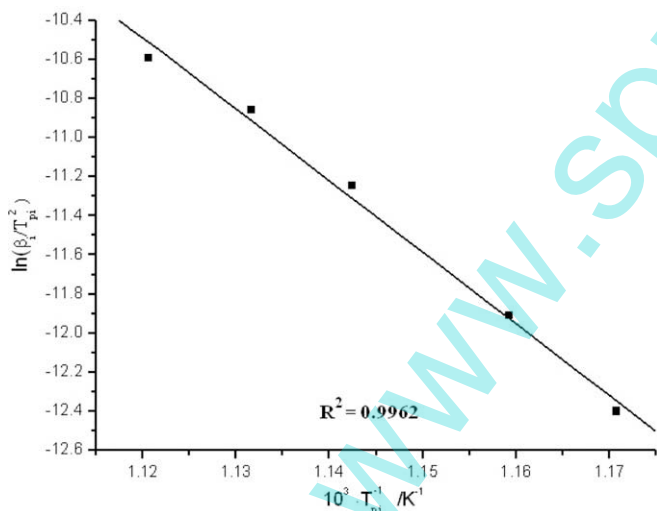| Heating rate (β)/(K min^{-1})	3	5	10	15	20
Peak temperature (T_p)/K	854.1	862.6	875.3	883.7	892.4
$10^3 \times (1/T_p)$	1.171	1.159	1.142	1.132	1.121
$\ln(\beta/T_p^2)$	−12.401	−11.910	−11.247	−10.860	−10.592

Fig. 13. Fitting lines by Kissinger method.

Table 2
Specific surface area as a function of firing temperature.

Temperature (°C)	400	700	1000
Specific surface area (m^2/g)	197	112	75

4. Conclusion

In summary, nanosized cobalt aluminate particles were synthesized using a precursor method with the aid of ultrasound irradiation under various preparation parameters. The precursor on heating yields nanosized CoAl$_2$O$_4$ particles. The effects of the preparation parameters, such as the sonochemical reaction time and temperature, precipitation agents, calcination temperature and time on the formation of CoAl$_2$O$_4$ were investigated. The precursor and the nanoparticles were characterized by an array of experimental techniques. The use of ultrasound irradiation during the homogeneous precipitation of the precursor reduces the duration of the precipitation reaction duration of the precursor. The mechanism of the formation of cobalt aluminate was investigated by means of Fourier transformation infrared spectroscopy (FT-IR) and EDX (energy dispersive X-ray). The thermal decomposition process and kinetics of the precursor of nanosized CoAl$_2$O$_4$ were investigated by means of differential scanning calorimetry (DSC) and thermogravimetry (TG). The apparent activation energy (E) is 304.26 kJ/mol and the pre-exponential constant (A) is 6.441×10^{14} s^{-1}. Specific surface area was investigated by means of Brunauer Emmett Teller (BET) surface area measurements. Mono-phasic cobalt aluminate with a crystallite diameter of 20 nm along the (3 1 1) plane was formed when the products were synthesized using Co(NO$_3$)$_2$·6H$_2$O and Al(NO$_3$)$_3$·9H$_2$O as starting materials, with urea as a precipitation agent. The reaction was carried out under ultrasound irradiation at 70 °C for 4 h and a calcination temperature of 1000 °C for 6 h.

References

[1] K.S. Suslick, S.B. Choe, A.A. Cichowlas, M.W. Grinstaff, Nature 353 (1991) 414.
[2] A. Gedanken, Ultrason. Sonochem. 11 (2004) 47.
[3] A.E. Kandjani, M.F. Tabriz, B. Pourabbas, Mater. Res. Bull. 43 (2008) 645.
[4] A. Troia, M. Pavese, F. Geobaldo, Ultrason. Sonochem. 16 (2009) 136.

[5] A.Y. Baranchikov, V.K. Ivanov, Y.D. Tretyakov, Ultrason. Sonochem. 14 (2007) 131.
[6] R. Xie, D. Li, H. Zhang, M. Jiang, T. Sekiguchi, B. Liu, Y. Bando, J. Phys. Chem. B 110 (2006) 19147.
[7] X.K. Wang, G.H. Chen, W.L. Guo, Molecules 8 (2003) 40.
[8] I.K. Kim, S.J. Yoa, J.K. Lee, C.P. Huang, Korean J. Chem. 20 (2003) 1045.
[9] D.S. Jacob, V. Kahlenberg, K. Wurst, L.A. Solovyov, I. Felner, L. Shimon, H.E. Gottlieb, A. Gedanken, Eur. J. Inorg. Chem. (2005) 522.
[10] Y.B. Alexander, K.I. Vladimir, Y.D. Tretyakov, Ultrason. Sonochem. 14 (2007) 131.
[11] I.C. Halalay, M.P. Balogh, Ultrason. Sonochem. 15 (2008) 684.
[12] Q.Y. Li, X.L. Zhang, G.Z. Wu, S.A. Xu, C.F. Wu, Ultrason. Sonochem. 14 (2007) 225.
[13] Y.C. Han, S.P. Li, X.Y. Wang, I.G. Bauer, M.Z. Yin, Ultrason. Sonochem. 14 (2007) 286.
[14] J. Pinkas, V. Reichlova, R. Zboril, Z. Moravec, P. Bezdicka, J. Matejkova, Ultrason. Sonochem. 15 (2008) 257.
[15] H.Y. Zheng, M.Z. An, J. Alloy. Compd. 459 (2008) 548.
[16] S.D. Lepore, Y. He, J. Org. Chem. 68 (2003) 6261.
[17] D. Mazza, A. Delmastro, S. Ronchetti, J. Eur. Ceram. Soc. 20 (2000) 699.
[18] N. Ouahdi, S. Guillemet, B. Durand, J. Eur. Ceram. Soc. 28 (2008) 1987.
[19] W.S. Cho, M. Kakihana, J. Alloy. Compd. 287 (1999) 87.
[20] D.M.A. Melo, J.D. Cunha, J.D.G. Fernandes, Mater. Res. Bull. 38 (2003) 1559.
[21] N. Ouahdi, S. Guillemet, J.J. Demai, Mater. Lett. 59 (2005) 334.
[22] G. Carta, M. Casarin, N.E. Habra, Electrochim. Acta 50 (2005) 4592.
[23] P.H. Bolt, F.H.P.M. Habraken, W.F. Geus, J. Solid State Chem. 135 (1998) 59.
[24] S. Chokkaram, R. Srinivasan, D.R. Milburn, B.H. Davis, J. Catal. A: Chem. 121 (1997) 157.
[25] W.S. Cho, M. Kakihana, J. Alloy. Compd. 87 (1999) 87.
[26] S. Chemlal, A. Larbot, M. Persin, Mater. Res. Bull. 35 (2000) 2515.
[27] M. Sales, K. Valentin, J. Alarcon, J. Eur. Ceram. Soc. 17 (1997) 41.
[28] C.O. Arean, M.P. Mentruit, E.E. Platero, Mater. Lett. 39 (1999) 22.
[29] S. Kurajica, E. Tkalcec, J. Schmauch, J. Eur. Ceram. Soc. 27 (2007) 951.
[30] M. Zayat, D. Levy, Chem. Mater. 9 (2000) 2763.
[31] U.L. Stangar, B. Orel, M. Krajnc, Mater. Tech. 36 (2002) 387.
[32] Z.Z. Chen, E.W. Shi, W.J. Li, Mater. Lett. 55 (2002) 281.
[33] Z.Z. Chen, E.W. Shi, W.J. Li, Mater. Sci. Eng., B 107 (2004) 217.
[34] W.D. Li, J.Z. Li, J.K. Guo, J. Eur. Ceram. Soc. 23 (2003) 2289.
[35] W.Z. Lv, Z.K. Luo, H. Yang, Ultrason. Sonochem. 17 (2010) 344.
[36] W.Z. Lv, B. Liu, Q. Qiu, J. Alloy. Compd. 479 (2009) 480.
[37] W.Z. Lv, B. Liu, Z.K. Luo, J. Alloy. Compd. 465 (2008) 261.
[38] W.Z. Lv, Z.K. Luo, B. Liu, Key Eng. Mater. 368 (2008) 604.
[39] W.Z. Lv, B. Liu, Z.K. Luo, J. Mater. Sci. Eng. 25 (2007) 686.
[40] W.Z. Lv, Z.K. Luo, P.X. Zhang, Inorg. Chem. Ind. 39 (2007) 16.
[41] W.Z. Lv, B. Liu, S.H. Wei, J. Shenzhen Univ. 23 (2006) 329.
[42] P. Jeevanandam, Y. Koltypin, A. Gedanken, Mater. Sci. Eng., B 90 (2002) 125.
[43] W.B. McNamara, Y.T. Didenko, K.S. Suslick, Nature 401 (1999) 772.